Published in final edited form as:
Nanomedicine (Lond). 2013 May ; 8(5): 725–737. doi:10.2217/nnm.12.125.

Functional interaction between charged nanoparticles and cardiac tissue: a new paradigm for cardiac arrhythmia?

Michele Miragoli[#1,2], **Pavel Novak**[#1,3], **Pakatip Ruenraroengsak**[4], **Andrew I Shevchuk**[3,5], **Yuri E Korchev**[3], **Max J Lab**[1], **Teresa D Tetley**[4], and **Julia Gorelik**[*,1]

[1]Myocardial Function Unit, National Heart & Lung Institute, Imperial College London, 4th floor, Imperial Centre for Translational & Experimental Medicine, Hammersmith Campus, Du Cane Road, London, W12 0NN, UK

[2]Centre of Excellence for Toxicological Research, exISPESL- INAIL, Dept of Evolution & Functional Biology, Section of Physiology, University of Parma, 43124 Parma, Italy

[3]Division of Medicine, Imperial College London, Du Cane Road, London, W12 0NN, UK

[4]Lung Cell Biology, Section of Pharmacology & Toxicology, National Heart & Lung Institute, Dovehouse Street, Imperial College London, London, SW3 6LY, UK

[5]Institute for Life Sciences, University of Southampton 3046, Life Sciences Building 85, Highfield, Southampton, SO17 1BJ, UK

[#] These authors contributed equally to this work.

Abstract

Aim—To investigate the effect of surface charge of therapeutic nanoparticles on sarcolemmal ionic homeostasis and the initiation of arrhythmias.

Materials & methods—Cultured neonatal rat myocytes were exposed to 50 nm-charged polystyrene latex nanoparticles and examined using a combination of hopping probe scanning ion conductance microscopy, optical recording of action potential characteristics and patch clamp.

Results—Positively charged, amine-modified polystyrene latex nanoparticles showed cytotoxic effects and induced large-scale damage to cardiomyocyte membranes leading to calcium alternans and cell death. By contrast, negatively charged, carboxyl-modified polystyrene latex nanoparticles

[*]Author for correspondence: Tel.: +44 2075942736, Fax: +44 20 7594 3653, j.gorelik@ic.ac.uk.

Financial & competing interests disclosure
The authors are supported by the following funds: Medical Research Council UK grant no. G0700926 to TD Tetley, YE Korchev and J Gorelik; Wellcome Trust grant no. WTN090594 to J Gorelik and M Miragoli; Young Researcher Project, Italian Ministry of Health grant no. GR-2009-1530528 to M Miragoli. P Novak, AI Shevchuk, YE Korchev and MJ Lab hold shares of Ionscope Ltd, UK, a small spin-out company manufacturing scanning ion conductance microscopes. The authors have no other relevant affiliations or financial involvement with any organization or entity with a financial interest in or financial conflict with the subject matter or materials discussed in the manuscript apart from those disclosed.
No writing assistance was utilized in the production of this manuscript.

Ethical conduct of research
Isolation procedures from 1-day-old Wistar rats were in accordance with the guidelines of the UK Home Office Animal (Scientific Procedures) Act 1986. The authors state that they have obtained appropriate institutional review board approval or have followed the principles outlined in the Declaration of Helsinki for all human or animal experimental investigations. In addition, for investigations involving human subjects, informed consent has been obtained from the participants involved.

Europe PMC Funders Author Manuscripts

(NegNPs) were not overtly cytotoxic but triggered formation of 50–250-nm nanopores in the membrane. Cells exposed to NegNPs revealed pro-arrhythmic events, such as delayed afterdepolarizations, reduction in conduction velocity and pathological increment of action potential duration together with an increase in ionic current throughout the membrane, carried by the nanopores.

Conclusion—The utilization of charged nanoparticles is a novel concept for targeting cardiac excitability. However, this unique nanoscopic investigation reveals an altered electrophysiological substrate, which sensitized the heart cells towards arrhythmias.

Keywords

action potential; arrhythmia; calcium transient; cardiac electrophysiology; cell topography; conduction velocity; DADs; electrically charged nanoparticles; nanopores; scanning ion conductance microscopy

Cardiovascular disease has long been the foremost reason for death in developed countries and is becoming the number one killer in developing countries [1].

Conventional pharmacological therapy is largely ineffective and there is much effort in the field of nanomedicine where nanoparticles (NPs) may play a pivotal role in drug delivery. Epidemiological studies have linked very small particles in air pollution with cardiovascular and respiratory mortality and morbidity [2,3]. Prior studies have found that particulate matter (PM) affects cardiac performance and in particular ultrafine particles may cause heart rate variability [4,5] and arrhythmia [6]. Thus, with the implementation of the Clean Air Act in the USA [7], the WHO has endeavored to improve air quality worldwide. One metric is PM less than 10, 2.5 and 0.1 μm in aerodynamic diameter. Although it is difficult to monitor particles within the nanometer range, increasing evidence supports a role for NPs (PM <100 nm) in increased morbidity and mortality, even when pollution levels are below government standards for clean air quality [8]. A correlation exists between inhaled NPs and heart rate variability and ectopy, supported by *in vivo* [9] and *ex vivo* [10] studies.

Nevertheless, in the face of the development of NP drug delivery systems, there is a pressing need to better understand NP interactions within the body and, in the light of the PM studies, particularly in the cardiovascular system, where possible effects of pro- or anti-arrhythmic events caused by NPs are unknown.

Since one route of delivery of nanoparticulate drugs to the vasculature is via inhalation, it is of note that electrically charged NPs with a hydrodynamic diameter between 6 and 34 nm can cross the pulmonary alveolar epithelial barrier and may eventually enter the systemic circulation [11], potentially having a direct adverse effect on the cardiovascular system [12]; release of prothrombotic and inflammatory cytokines by the lung may set up a cascade of vascular reactivity. Such events could result in electrical desynchronization of cardiac activity and autonomic function [13]. Another proposed mechanism underpins that NPs derived from diesel exhaust PM play a role in the inflammatory process by enhancing oxidative stress [14,15]. Neither of these explanations considers the physicochemical nature of the NPs.

Europe PMC Funders Author Manuscripts

Europe PMC Funders Author Manuscripts

NPs in urban air, for example, are highly heterogeneous; the majority are emitted from diesel exhausts, with a primary aerodynamic diameter of approximately 20 nm and are electrically charged [16]. Currently, it is not known whether the surface charge of such NPs could affect an electrically excitable tissue such as cardiac tissue. To address this hypothesis, the effect of positively and negatively charged NPs on neonatal rat ventricular myocytes was evaluated. We analyzed not only the classic mechanism of cardiotoxicity (i.e., apoptosis and necrosis) but also a direct interaction of excitable cardiac membrane and charged NPs that leads to electrophysiological changes in cardiac excitability. The results will open a new perspective to understand the pro-arrhythmic risk for the NP–cardiac tissue interaction, depending on surface charge.

Materials & methods

A detailed ‘methods section’ is provided in Appendix 1.

Cell culture of neonatal rat ventricular cardiomyocytes

Preparations consisted of single cells, clusters (5–10 cells) or long linear 80 μm width × 1 cm long strands (courtesy of Stephan Rohr, University of Bern, Switzerland) of neonatal rat ventricular cardiomyocytes (NRVMs), obtained using previously described techniques [17,18]. Experiments were performed with 3–4-day old preparations.

Optical measurement of electrical activity & intracellular calcium transient

Measurements of electrical activity and intracellular calcium (Ca_i^{2+}) transients were performed using an inverted microscope Nikon TEi in conjunction with a fast CMOS camera (MiCAMUltima, Scimedia) at 20× and 40× magnification, depending upon the type of experiment [19,20]. Preparations were mounted in a temperature-controlled experimental chamber and transferred to the stage of an inverted microscope equipped for epifluorescence. Preparations were stained for 4 min with the voltage-sensitive dye di-8-ANEPPS (135 μmol/l, Biotium) or 20 min with Fluo-4 FF (5 μmol/l, Invitrogen) and superfused at 36°C with Hank’s balanced salt solution (HBSS; pH 7.4, Sigma). Electrical activity was recorded for 2 s (di-8-ANEPPS) or 4 s (Fluo-4 FF) in order to minimize phototoxicity. Individual strands and clusters for impulse propagation and APD_{90} measurement were stimulated with a bipolar electrode consisting of a glass micropipette filled with HBSS and a silver wire coiled around the shank as previously described [21]. The stimulation electrode was placed 1-mm apart from the measurement site in order to permit propagation to reach a steady state. Preparations were pre-stimulated for 10 s at 2 Hz (SD9, Grass Instruments) before recording a single propagated action potential (AP). AP duration (APD) was calculated at 90% of repolarization.

Hopping probe ion conductance microscopy

All hopping probe scanning ion conductance microscopy (HPICM) experiments were performed using a custom modified ICnano S scanner (Ionscope Ltd) described previously [22]. Scanning nanopipettes of approximately 200 MΩ resistance were pulled from borosilicate glass with an outer diameter of 1 mm and inner diameter (ID) of 0.5 mm (Intracell) using a laser puller P-2000 (Sutter Instr. Co.). Nanopipettes were filled with PBS

and had an estimated ID of approximately 50 nm. For acute exposure, NPs were applied via another pipette with an approximately 1.5-μm ID tip positioned close to the cardiomyocyte.

Patch-clamp recordings

All whole-cell patch-clamp recordings were made with a custom modified ICnano S scanner using the patch-clamp amplifier Axopatch 200B (Molecular Devices) and digitized using Digidata 1322A (Molecular Devices) and Clampex 9.2 (Molecular Devices). In the real-time recording of membrane current, 50-nm negatively charged, carboxyl-modified polystyrene latex NPs (NegNPs) were applied via another pipette positioned close to the cardiomyocyte.

Particle size & ζ-potential

Latex polystyrene 50-nm NPs, both NegNPs and positively charged, amine-modified polystyrene latex NPs (PosNPs) were purchased from Sigma. These NPs were used as models for both NP-based drug delivery systems and PM ($P.M_{0.1}$). NPs were suspended in distilled water and M199 tissue culture medium at a final concentration of 10 μg/ml. NPs were vortexed and filtered through a 0.22-μm membrane filter. The samples were sonicated in a sonicating water bath for 2 min just prior to measuring size and ζ-potential using a Zetasizer Nano (Malvern Instruments Ltd).

Particle uptake observed by transmission electron microscopy

After the exposure, the cells were rinsed with PBS and fixed with 2.5% glutaraldehyde for 2 h. The samples were post-fixed in 1% osmium tetroxide for 15–30 min. The samples were dehydrated, for 15 min each, in 70% ethanol (1×), 90% ethanol (1×) and 100% ethanol (3×), respectively, at room temperature.

Fifty percent araldite agar in ethanol was added to each well and incubated for 15 min, each at room temperature before changing to 100% araldite agar. The specimens were then embedded into araldite agar. The beam capsule embedding the cell monolayer was cut on microtome, using a glass knife, into ultra-thin slices, 0.05–0.20 μm in width. The obtained sections were stained with 1.5% uranium acetate and 5% lead citrate before viewing under transmission electron microscopy (TEM). Up to 100 cells (nine sections for each NP exposure recruited from three nonoverlapping sections were cut from the embedding block: three blocks came from three separate experiments [n = 3]) were analyzed by TEM for uptake of each type of NPs and the percentage of cells which took up NPs were calculated.

Data analysis

Data obtained with the macroscopic imaging system were analyzed using proprietary software (Brainvision, version 10.08, Scimedia). Topography data were processed using custommodified ICnano S scanner controller software.

Statistics

Data were compared using the Student’s t test (two-tailed; heteroscedastic). Differences were considered significant at $*p < 0.05$ and $**p < 0.001$ (mean ± SD) for all figures. The data obtained from cell-based assays (except NP uptake data) were analyzed by two-way and

factorial ANOVA analysis using SPSS package software (SPSS 17.0) with *post hoc* test (Bonferroni) for multiple comparisons.

Results

Internalization of charged NPs

We studied the consequence of exposure of primary NRVMs to electrically charged NPs of approximately 50-nm hydrodynamic diameter (Figure 1A & Supplementary Figure 1; see online at www.futuremedicine.com/doi/full/10.2217/nnm.12.125) on cell viability *in vitro,* using the MTT assay (Figure 1B). NegNPs did not induce cell death; the viability was approximately 90% after 4 h exposure (particle concentration: 0–300 μg/ml). By contrast, PosNPs induced 60% cell death at 50 μg/ml, by 4 h exposure. Accordingly, TEM demonstrated that PosNPs penetrated (~89% cell uptake) the membrane [23] of NRVMs and induced breakdown of mitochondria and myofibril networks (Figure 1C, control vs Figure 1DI & DII), whereas NegNPs predominantly adhered to the cell membrane (~90%); approximately 60% of the NegNPs remained associated with the cell membrane, while approximately 30% were eventually internalized by the cells at 4 h (Figure 1Ei).

Cardiotoxicity of positively charged NPs

We recorded Ca_i^{2+} transient and transmembrane voltage characteristics in clusters of NRVMs (three to five cells) following exposure to PosNPs (2 and 4 h) (Figure 2), using an inverted fluorescence microscope equipped with a high-resolution camera. There was a significant percentage of cells that formed Ca_i^{2+} alternant clusters at 2 and 4 h exposure (maximum peak at 20 μg/ml, ~70% of the total clusters, 2 h exposure) (Figure 2A & C).

The recording of optical transmembrane potential revealed that the AP shape and duration and the spontaneous beating rate at different exposure times were unaffected (Figure 2B & C). AP duration, calculated at 90% of repolarization (APD_{90}) ranged from 180 ± 36 ms (control) to 268 ± 68 ms (4 h exposure; not significant) and the spontaneous beating rate ranged from 126 ± 8 bpm (control) to 123 ± 25 bpm (4 h exposure; not significant).

HPICM is a technique that permits topographical reconstruction of the membrane surface of living cells at nanometer resolution [20,24]. Using this technique, we found that NRVMs exposed to PosNPs exhibited localized membrane disruption (Figure 2D, E & G), accompanied by general necrosis and apoptosis, confirmed by propidium iodide uptake, annexin V staining (Figure 3A & B) and caspase-3 activity assay (data not shown). By contrast, NegNPs showed only marginal staining of propidium iodide (Figure 3A–C). The effect of NPs at a concentration range below 10 μg/ml was also analyzed and neither type of NPs showed statistical significance (data not shown).

Negatively charged NPs alter AP properties

After exposure to NegNPs for 2 h, NRVMs appeared viable; there was only marginal staining for propidium iodide uptake and annexin V (Figure 3A–C). Interestingly, optical AP measurements denoted a delayed afterdepolarization (DAD, Figure 4A, 2 h), with a marked significant reduction of AP amplitude after 4-h exposure. There was a significant dose-

dependent increment in APD_{90} from 174 ± 25 ms (control) to 430 ± 93 ms (50 μg/ml, r^2 = 0.86, 2 h) (Figure 4B) between 2 and 4 h of exposure, accompanied by a reduction in the rate of spontaneous beating from 120 ± 12 to 35 ± 9 bpm (r^2 = 0.87). These altered electrophysiological parameters are well-known pivotal scenarios for ventricular fibrillation [25]. Furthermore, Ca_i^{2+} transient was pathologically prolonged (67%) (Figure 4C) in the NegNP-exposed cells (341 ± 71 ms, control vs 503 ± 119 ms, 2 h).

Negatively charged NPs, calcium activity & transmembrane current

After 2 h of NegNP exposure, the NRVMs segregated into three groups according to different States of spontaneous Ca_i^{2+} activity (Supplementary Moive 1). In the first group (23% of clusters), the Ca^{2+} re-uptake was incomplete (Figure 4D) but a basal Ca_i^{2+} was still recorded in the cell; in the second group (23% of clusters) the basal Ca_i^{2+} was characterized by an ulterior transient increment, seen approximately 2 s following the first spontaneous complete Ca_i^{2+}. However, in the third group (44% of clusters, significant with respect to the other two groups), the increment of Ca_i^{2+} never ended; instead a persistent increment in Ca_i^{2+} was observed throughout the recording.

The relationship between the membrane potential and the ionic current flow through the membrane (I-V), in the presence of NegNPs, was measured in whole-cell patch clamp configuration (Figure 4E) using HPICM setup. We found a subpopulation of cells with significantly increased background current flow (-134.4 ± 37.5 pA at -70 mV) compared with that of the remaining cells (-31.9 ± 14.5 pA at -70 mV). The linear character of the I-V curve and reversal potential of -3.7 ± 2.6 mV suggested that in the NRVM NegNP-sensitive subpopulation, the change in membrane conductance was nonselective and voltage-independent. As exemplified in real-time recording from a single NRVM exposed to 10 μg/ml NegNPs (Figure 4F), the membrane current (I_M) started to increase in a step-wise manner before developing into a huge membrane leak of a few nanoamperes (nA) within 50 min of exposure.

Formation of nanopores in cardiac membranes

HPICM revealed randomly distributed nanopores with diameters ranging from 50 to 250 nm in NRVMs exposed for 4 h to NegNPs and subsequently fixed in formalin (Figure 5A & B & Supplementary Figure 2). We observed similar porous structures in the membranes of live, spontaneously contracting NRVMs after acute exposure (2 min) to NegNPs (Figure 5C), ruling out any potential role of the fixative in the development of membrane pores detected in fixed cells.

NegNPs affect conduction velocity

We assessed cardiac impulse propagation optically, in defined patterned growth NRVM cultures (Figure 6A). The pattern consisted of individual strands of confluent NRVMs, 80 μm by 10 mm. The preparations were stimulated at 2 Hz as previously described [17] and the AP propagation characteristics were recorded at 10 kHz. We found a significant reduction in conduction velocity from 32.3 ± 2.9 cm/s (control) to 20.0 ± 3.1 cm/s (NegNPs, 50 μg/ml, 2 h)(Figure 6B).

Discussion

Charged NPs & cardiomyocytes: an electrical interface

Our results show that there is an interaction between the surface charge of the NPs and NRVMs, possibly reflecting the excitable nature of the heart. The most important finding in these observations is that NegNPs, even if not as cytotoxic as PosNPs, can also induce arrhythmias in NRVMs. Despite this, a similar approach in imaging NPs has been demonstrated previously [23,26], where we combined HPICM and electrophysiological techniques for monitoring the functional effect of charged NPs on cardiac tissue. A dose of 10 μg/ml PosNPs preferentially penetrated the cells and induced apoptosis and necrosis within 4 h of exposure. We previously showed that exposure of engineered homocellular confluent strands of NRVM [27] to diesel exhaust particles altered the AP characteristics, disrupting myofibril organization and inducing oxidative stress [21]. Importantly, several organometallic NPs ranging from 20 to 50 nm are present in diesel lubricants [16,28], are electrically charged and may be harmful to the population exposed.

Consequences of exposure to PosNPs on the structure & function of NRVM

Cells in the clusters seem to be unevenly exposed to PosNPs; therefore, increasing the concentration of particles from 20 to 50 μg/ml did not lead to a substantial increase in the number of affected clusters. Interestingly, it was still possible to study AP in some clusters beyond 4 h exposure to PosNPs, despite the fact that apoptosis and necrosis occurred much earlier in other affected clusters. The number of PosNP hits was probably less in those that were least affected; this could explain why the APD_{90}, after 4 h exposure to PosNPs, was similar to the control, in view of the fact that not all the clusters were exposed to PosNPs at the same magnitude. Such a non-uniform effect could be due to aggregation or agglomeration of the PosNPs via the interaction between PosNPs and proteins in M199 media. This can be seen from the increase in polydispersity index value (PDI) in Figure 1A, the reduction of surface charge density of both types of NPs (Supplementary Figure 1) and a broadening of the size distribution curve (Supplementary Figure 1C & D). Although a significant increase in the PDI value of NegNPs was also found, the increase in particle size of the NegNPs was not found to be significant. We recently reported the effect of proteins in media that could cause a reduction in ζ-potential value and biological activity of the same particles in different types of media [23]. The aggregation of PosNPs in M199 media will decrease the number of single PosNPs available for exposure to the cells. However, the internalization of PosNPs induced, acutely, a ‘woodworm’-like membrane disruption; indeed, during the early exposure (2 h) characterized by necrotic and apoptotic processes, we observed a significant dose-response increase in the percentage of Ca_i^{2+} alternans in NRVM clusters after 2 h exposure, which was not the case for clusters that were exposed to PosNPs for a longer duration, for example, 4 h. This discrepancy could be because of inhomogeneous particle distribution, where highly concentrated particle-cell hits induced cell death after 4 h, whilst we detected optically the physiological Ca_i^{2+} transient mainly from the surviving, possibly less exposed clusters.

NegNPs affect AP characteristics & membrane excitability

The diffusion of negatively charged NPs was also probably not homogeneous; however, they preferentially adhered to the sarcolemma and the cells did not undergo necrosis and minimal apoptotic processes were detectable after 4 h. We found that NegNPs were highly pro-arrhythmogenic, inducing DADs, APD_{90} prolongation, Ca_i^{2+} overload and reducing cellular beating rate and conduction velocity. The observed effects can be explained by an ionic current leak throughout the life-compatible nanopores, as observed in the patch-clamp experiments.

In order to circumvent the possibility that NegNPs did not adhere to the patched cells, we performed local application of NegNPs with a second nanopipette close to the patch-clamp pipette. We found that after local NegNP administration, I_M drastically increased over 50 min, in a step-wise manner, reminiscent of the behavior of I_M observed during formation of membrane pores, or switching of ion channels between different conducting states [29].

Life-compatible nanopore formation

NegNPs, by inducing nanopores, alter the electrical function of the sarcolemma and therefore the cardiac excitability; this explains the Ca_i^{2+} overload, the APD prolongation and, to some extent, the reduction of the beating rate of NRVM. Moreover, the conduction velocity was significantly reduced; we speculate that the Ca^{2+} overload may influence the appropriate extrusion mechanisms of Ca^{2+} ions [30] (via the stoichiometry of Na/Ca exchange), which may indirectly reduce the amount of Na current availability. We have previously reported that PosNPs at 50 μg/ml demonstrated a toxic effect on transformed human alveolar epithelial type 1-like (TT1) cells [23] by initiating the nanopore formation in cell membranes in parallel with a significant increase in the release of lactate dehydrogenase (LDH), normally sequestered inside cells to culture media, indicating severe plasma membrane damage following 4 h exposure. However, the NegNPs were not found to be toxic to TT1 cells. The variation between these two experiments indicated two key parameters that must be measured during the study of the interaction between NPs and the cells – surface charge density of NPs in exposure medium and cell membrane potential.

Conclusion

On the basis of *in vivo* studies, the perspective that emerges is should heart tissue be directly exposed to circulating NPs, there could be more rapid induction of arrhythmogenesis than had previously been considered likely (short-term exposure, i.e., hours to days) [13,31,32]. Our data demonstrate that NegNPs can induce arrhythmogenic effects in NRVM, even without penetrating the cell, possibly due to pore formation in exposed membranes. The effect of NegNPs is not uniform and the quality of the electrical isolation barrier of the lipid bilayer is compromised by a nonspecific conductance. Germane to this, an ionic leak through such nanopores may provide an obvious explanation for the desynchronization of the calcium-induced calcium-release mechanism, as well as prolongation of APD_{90} and DADs.

Limitations

Nanopores formed by NegNPs apparently do not kill NRVMs in the short term; however, it is currently unclear whether nanopore formation is transient in the membrane and compatible with cell survival. More long-term HPICM topographical experiments (images taken for 24 h) describing the life-time for NRVMs are needed to answer this question. To be able to predict how PosNP and NegNP exposure may affect cardiac function *in vivo,* several limitations of the studies with cultured cells need to be addressed. First, investigations of cultured cells are conducted in serum-free medium whereas *in vivo,* cells are exposed to serum proteins. NPs tend to rapidly adsorb protein for the surrounding environment [33] resulting in an alteration of the surface charge and therefore subsequent interaction with cells may be altered. Second, the pulmonary barrier limits airborne NP translocation from the lung into the circulation [11] and third, people will have variable exposure to NPs depending on their occupation, socioeconomic status and the location in which they live (urban and suburban traffic exposure may be different).

Recently it has been shown in a model of *ex vivo* Langerdorff perfused heart that engineered NPs affect heart rate [10]; however, further *in vivo* animal experiments are required to assess the exact impact of NPs upon this likelihood, especially in the context of ambient aerosol NPs.

Future perspective

In this study we have considered the development of pores and induction of arrhythmogenesis in terms of putative nanopore cytotoxicity; however, in the emerging field of nanomedicine the presence and the control of such nanopore formation might be clinically relevant for drug delivery and cardiac rhythm management. Further prospective studies are needed to provide evidence-based data to support this treatment option in cardiovascular diseases. Nonetheless, both PosNPs and NegNPs are arrhythmogenic and in several circumstances (infarct and ischemia) may induce re-entry circuits; indeed epidemiological study indicates that people with coronary artery disease and heart failure are more susceptible to air pollution. A key investigation would be to define the interaction between infarct tissue and charged NPs since fibrotic areas are themselves pro-arrhythmogenic, but the additional interaction with NPs may well raise the likelihood of arrhythmic events.

Supplementary Material

Refer to Web version on PubMed Central for supplementary material.

Acknowledgements

The authors thank S Rohr for kindly providing pattern growth coverslips for the experiments and AV Rogers (EM Unit, Royal Brompton Hospital, London, UK) for proficient assistance with electron microscopy.

Appendix 1: Nanoparticle exposure

NRVMs were seeded at a density of 0.15 to 1.5 × 10^3 cells/mm^2 on 22 mm-diameter round coverslips (optical recording, topography and patch-clamp experiments) or at 2.5 × 10^4 cells/well in 24-well plates for toxicological investigation. At 48 h, the cells were exposed to serum-free medium containing nanoparticles (NPs) at concentrations of 0, 1, 10, 25, 50, 100 and 250 μg/ml, for 2–4 h at 37°C. NPs were suspended in serum-free M199 (Sigma Aldrich) and sonicated in a sonicating water bath for 2 min before adding to the cells.

In some topographical experiments (HPICM), cardiomyocytes were fixed in 4% formaldehyde after the incubation in order to obtain high-resolution images free of artifacts induced by spontaneous contractions.

Cell viability (MTT assay)

Following the 4 h exposure period, the medium was removed, the cells were thoroughly washed with PBS to remove residual NPs and then incubated with 3-(4,5-Dimethylthiazol-2-yl)-2,5-diphenyltetrazolium bromide (MTT) in fresh medium, 50 μg/ml, for 2.5 h at 37°C. The medium was removed and 200 μl of DMSO was added in each well to dissolve the cells and the insoluble formazan dye. The plate was placed on a rotary shaker and centrifuged at 14,000 g for 20 min to remove any residual NPs, before reading the optical density of the supernatants using a Thermomax microplate reader at 570 nm (MTX Lab Systems). The viability of the cells exposed to NPs was then calculated as a percentage of the unexposed control cells (exposed to PBS vehicle). To determine the effect of NPs they were either added to unexposed, control cells immediately before the MTT assay, or were added to the assay system following DMSO dissolution, and then processed identically to NP-exposed cells. Centrifugation at 14,000 g to remove the NPs from suspension was carried out prior to determination of the optical density of the supernatant, to avoid interference by NPs of the spectrophotometric assay.

Annexin V & propidium iodide staining

After 4 h NP exposure, the cells were rinsed and fixed with 2.5% paraformaldehyde in PBS for 10 min. Cells were then rinsed with PBS and stained with annexin V and propidium iodide (20 μg/ml) following the manufacturer’s protocol (BD Biosciences Pharmingen).

Caspase-3 activity

NP exposure was performed as described above and cells were analyzed at 1, 2 and 4 h. The medium was removed and the cells washed with PBS. Cell lysis buffer was added and the cell lysate was collected prior to analysis for caspase-3 using a commercial ELISA technique (DuoSet ELISA kits, R&D systems).

Whole-cell patch clamp

Patch-pipettes were pulled from borosilicate glass with an OD of 1.0 mm and ID of 0.5 mm (Sutter Inc.) using a laser puller P-2000 (Sutter Inc.). Pipette filling solution contained 120

mM K-Gluconate, 10 mM NaCl, 1 mM $CaCl_2$, 10 mM EGTA, 3 mM MgATP and 5 mM HEPES (pH = 7.2 [KOH]). HBSS with calcium and magnesium (Gibco, Invitrogen) was used as the bath solution. The patch-pipette resistance ranged from 6 to 9 MΩ when filled with pipette filling solution and immersed in HBSS.

Particle size & ζ-potential

Latex polystyrene 50 nm NPs – negatively charged carboxyl-modified NPs and positively charged amine-modified NPs – were purchased from Sigma Aldridge. NPs were suspended in distilled water and M199 tissue culture medium at a final concentration of 10 μg/ml. NPs were vortexed and filtered through a 0.22 μm membrane filter. The samples were sonicated in a sonicating water bath for 2 min just prior to measuring size and ζ-potential using a Zetasizer Nano (Malvern Instrument Ltd).

References

Papers of special note have been highlighted as:

■ of interest

1. Gersh BJ, Sliwa K, Mayosi BM, Yusuf S. Novel therapeutic concepts: the epidemic of cardiovascular disease in the developing world: global implications. Eur Heart J. 2010; 31(6):642–648. [PubMed: 20176800]
2. Nurkiewicz TR, Porter DW, Barger M, Castranova V, Boegehold MA. Particulate matter exposure impairs systemic microvascular endothelium-dependent dilation. Environ Health Perspect. 2004; 112(13):1299–1306. [PubMed: 15345343]
3. Nurkiewicz TR, Porter DW, Hubbs AF, et al. Nanoparticle inhalation augments particle-dependent systemic microvascular dysfunction. Part Fibre Toxicol. 2008; 5:1. [PubMed: 18269765]
4. Schulz H, Harder V, Ibald-Mulli A, et al. Cardiovascular effects of fine and ultrafine particles. J Aerosol Med. 2005; 18(1):1–22. [PubMed: 15741770]
5. Eninger RM, Rosenthal FS. Heart rate variability and particulate exposure in vehicle maintenance workers: a pilot study. J Occup Environ Hyg. 2004; 1(8):493–499. [PubMed: 15238301]
6. Sarnat SE, Suh HH, Coull BA, Schwartz J, Stone PH, Gold DR. Ambient particulate air pollution and cardiac arrhythmia in a panel of older adults in Steubenville, Ohio. Occup Environ Med. 2006; 63(10):700–706. [PubMed: 16757505]
7. Samet JM. The clean air act and health – a clearer view from 2011. N Engl J Med. 2011; 365(3): 198–201. [PubMed: 21732828]
8. Ware JH. Particulate air pollution and mortality – clearing the air. N Engl J Med. 2000; 343(24): 1798–1799. [PubMed: 11114320] [■ **Pioneering work that illustrates the problems regarding the effects of fine particle matter ($PM_{2.5}$) on health.**]
9. Wold LE, Simkhovich BZ, Kleinman MT, et al. *In vivo* and *in vitro* models to test the hypothesis of particle-induced effects on cardiac function and arrhythmias. Cardiovasc Toxicol. 2006; 6(1):69–78. [PubMed: 16845184]
10. Stampfl A, Maier M, Radykewicz R, Reitmeir P, Gottlicher M, Niessner R. Langendorff heart: a model system to study cardiovascular effects of engineered nanoparticles. ACS Nano. 2011; 5(7): 5345–5353. [PubMed: 21630684]
11. Choi HS, Ashitate Y, Lee JH, et al. Rapid translocation of nanoparticles from the lung airspaces to the body. Nat Biotechnol. 2010; 28(12):1300–1303. [PubMed: 21057497] [■ **Defines how nanosized particles (<50 nm) can rapidly translocate from the lung to the circulation**.]
12. Mills NL, Donaldson K, Hadoke PW, et al. Adverse cardiovascular effects of air pollution. Nat Clin Pract Cardiovasc Med. 2009; 6(1):36–44. [PubMed: 19029991]

13. Brook RD, Rajagopalan S, Pope CA 3rd, et al. Particulate matter air pollution and cardiovascular disease: an update to the scientific statement from the American Heart Association. Circulation. 2010; 121(21):2331–2378. [PubMed: 20458016]
14. Yokota S, Seki T, Furuya M, Ohara N. Acute functional enhancement of circulatory neutrophils after intratracheal instillation with diesel exhaust particles in rats. Inhal Toxicol. 2005; 17(12): 671–679. [PubMed: 16087573]
15. Okayama Y, Kuwahara M, Suzuki AK, Tsubone H. Role of reactive oxygen species on diesel exhaust particle-induced cytotoxicity in rat cardiac myocytes. J Toxicol Environ Health A. 2006; 69(18):1699–1710. [PubMed: 16864420]
16. Gidney JT, Twigg MV, Kittelson DB. Effect of organometallic fuel additives on nanoparticle emissions from a gasoline passenger car. Environ Sci Technol. 2010; 44(7):2562–2569. [PubMed: 20192164]
17. Miragoli M, Gaudesius G, Rohr S. Electrotonic modulation of cardiac impulse conduction by myofibroblasts. Circ Res. 2006; 98(6):801–810. [PubMed: 16484613]
18. Rohr S. Myofibroblasts in diseased hearts: new players in cardiac arrhythmias? Heart Rhythm. 2009; 6(6):848–856. [PubMed: 19467515]
19. Sheikh Abdul Kadir SH, Miragoli M, Abu-Hayyeh S, et al. Bile acid-induced arrhythmia is mediated by muscarinic M2 receptors in neonatal rat cardiomyocytes. PLoS ONE. 2010; 5(3):E9689. [PubMed: 20300620]
20. Miragoli M, Moshkov A, Novak P, et al. Scanning ion conductance microscopy: a convergent high-resolution technology for multi-parametric analysis of living cardiovascular cells. J R Soc Interface. 2011; 8(60):913–925. [PubMed: 21325316]
21. Helfenstein M, Miragoli M, Rohr S, et al. Effects of combustion-derived ultrafine particles and manufactured nanoparticles on heart cells *in vitro*. Toxicology. 2008; 253(1-3):70–78. [PubMed: 18824210]
22. Novak P, Li C, Shevchuk AI, et al. Nanoscale live-cell imaging using hopping probe ion conductance microscopy. Nat Methods. 2009; 6(4):279–281. [PubMed: 19252505] [■ **Demonstrates that further development of the scanning ion conductance microscope as a hopping probe microscope for studying cell membrane characteristics at the nanoscale range is needed**.]
23. Ruenraroengsak P, Novak P, Berhanu D, et al. Respiratory epithelial cytotoxicity and membrane damage (holes) caused by amine-modified nanoparticles. Nanotoxicology. 2012; 6(1):94–108. [PubMed: 21352086]
24. Nikolaev VO, Moshkov A, Lyon AR, et al. β2-adrenergic receptor redistribution in heart failure changes cAMP compartmentation. Science. 2010; 327(5973):1653–1657. [PubMed: 20185685]
25. Aiba T, Tomaselli GF. Electrical remodeling in the failing heart. Curr Opin Cardiol. 2010; 25(1): 29–36. [PubMed: 19907317]
26. Tetard L, Passian A, Venmar KT, et al. Imaging nanoparticles in cells by nanomechanical holography. Nat Nanotechnol. 2008; 3(8):501–505. [PubMed: 18685639]
27. Rohr S, Fluckiger-Labrada R, Kucera JP. Photolithographically defined deposition of attachment factors as a versatile method for patterning the growth of different cell types in culture. Pflugers Arch. 2003; 446(1):125–132. [PubMed: 12690471]
28. Vaaraslahti K, Keskinen J, Giechaskiel B, Solla A, Murtonen T, Vesala H. Effect of lubricant on the formation of heavy-duty diesel exhaust nanoparticles. Environ Sci Technol. 2005; 39(21):8497–8504. [PubMed: 16294893]
29. Cheek ER, Fast VG. Nonlinear changes of transmembrane potential during electrical shocks: role of membrane electroporation. Circ Res. 2004; 94(2):208–214. [PubMed: 14670844]
30. Sipido KR. Calcium overload, spontaneous calcium release, and ventricular arrhythmias. Heart Rhythm. 2006; 3(8):977–979. [PubMed: 16876751]
31. Chen J, Dong X, Zhao J, Tang G. *In vivo* acute toxicity of titanium dioxide nanoparticles to mice after intraperitioneal injection. J Appl Toxicol. 2009; 29(4):330–337. [PubMed: 19156710]
32. Burgan O, Smargiassi A, Perron S, Kosatsky T. Cardiovascular effects of sub-daily levels of ambient fine particles: a systematic review. Environ Health. 2010; 9:26. [PubMed: 20550697]

33. Oberdorster G, Oberdorster E, Oberdorster J. Nanotoxicology: an emerging discipline evolving from studies of ultrafine particles. Environ Health Perspect. 2005; 113(7):823–839. [PubMed: 16002369]

Europe PMC Funders Author Manuscripts

Europe PMC Funders Author Manuscripts

Executive summary

- Positively charged, amine-modified nanoparticles could penetrate into cardiomyocytes, by local disruption of the cell membrane.
- Positively charged nanoparticles induce necrosis, apoptosis and intracellular calcium alternans in cardiomyocytes.
- Negatively charged, carboxyl-modified nanoparticles could not penetrate into the cells and did not induce necrosis.
- High concentrations of negatively charged nanoparticles exhibited pro-arrhythmic events and induced a delayed afterdepolarization, action potential duration increment, the reduction of beating rates, incomplete calcium re-uptake and decrement in impulse propagation velocity.
- Negatively charged nanoparticles caused the formation of nanopores in the cell membrane that could influence ionic membrane conductance and thus modify cardiac excitability.

Europe PMC Funders Author Manuscripts

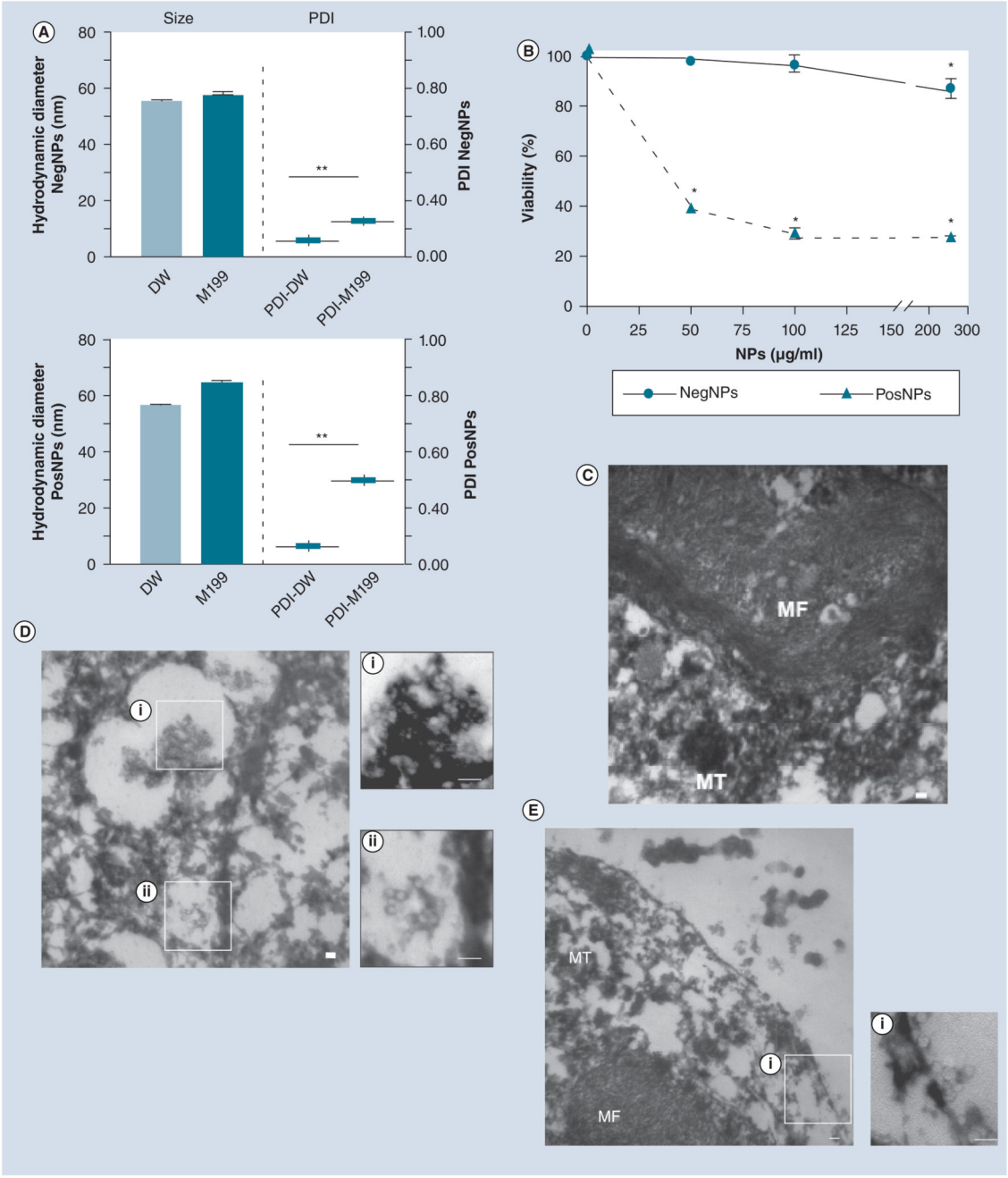

Figure 1. Interaction between 50-nm charged nanoparticles and cardiomyocyte membrane.

(A) Hydrodynamic diameter and PDI (mean ± standard deviation) of NegNPs (top) and PosNPs (bottom) in DW and M199 medium (n = 3; **p < 0.001). **(B)** Dose-dependent neonatal rat ventricular cardiomyocyte viability, exposed to NegNPs and PosNPs for 4 h (n = 3; *p < 0.05). **(C–E)** Transmission electron micrographs of the uptake of **(D)** PosNPs and **(E)** NegNPs by neonatal rat ventricular cardiomyocyte compared with **(C)** controls. **(C)** Cellular MF and the remaining MT were observed. Scale bar = 100 nm; n = 100. DW: Distilled water; MF: Myofibril; MT: Mitochondria; NegNP: Negatively charged, carboxyl-

modified polystyrene latex nanoparticle; PDI: Polydispersity index value; PosNP: Positively charged, amine-modified polystyrene latex nanoparticle.

Europe PMC Funders Author Manuscripts

Europe PMC Funders Author Manuscripts

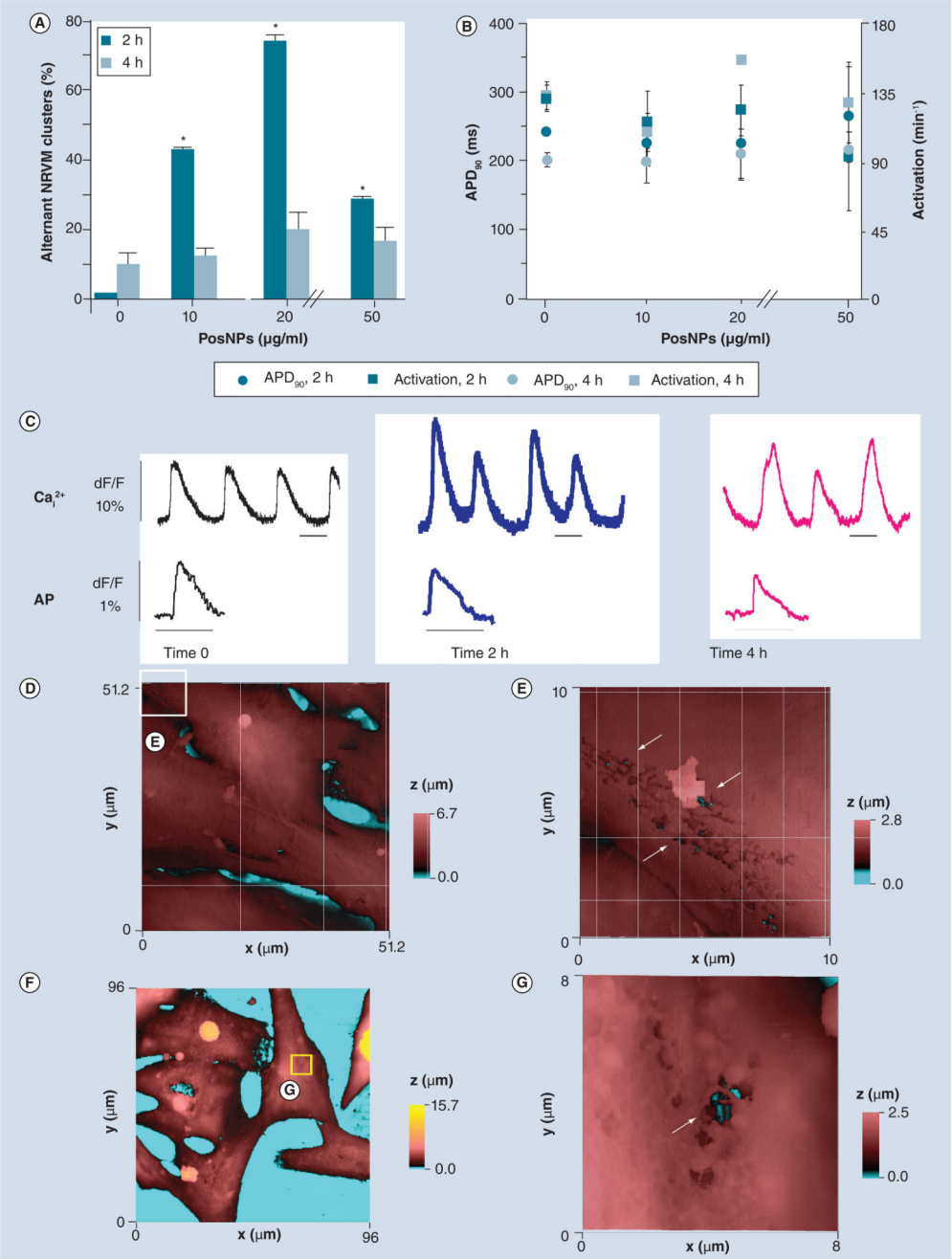

Figure 2. Electrophysiological and topographical investigation of cardiac cells subjected to positively charged, amine-modified polystyrene latex nanoparticles (facing page).

(A) Spontaneous alternans of beating clusters of NRVMs after 2-h and 4-h exposure to PosNPs ranging from 10 to 50 μg/ml (n = 22; mean ± standard deviation; *$p < 0.05$). **(B)** APD_{90} and spontaneous beats per minute (activation-1) recorded under the same conditions as **(A)** (n = 13; mean ± standard deviation). **(C)** Example of optical Ca_i^{2+} transient and AP traces recorded at time 0, after 2 and 4-h exposure to PosNPs. Scale bars = 500 ms. **(D)** Height-coded color topography image (51.2 × 51.2 μm) of NRVM fixed and imaged by

hopping probe scanning ion conductance microscopy after 4 h incubation with 50 μg/ml of PosNPs. **(E)** High-resolution topography (10 × 10 μm) of area depicted by the white square in **(D)** revealed membrane-breaching ‘woodworm’-like patterns in the membrane. Holes in the membrane (arrows) resulted from application of PosNPs exposing the interior, deep inside the cell (black and cyan colors). **(F)** Hopping probe scanning ion conductance microscopy image (96 × 96 μm) of live NRVMs after 2 h incubation with 50 μg/ml PosNPs. **(G)** High-resolution scan (8 × 8 μm) in the apparently unaffected area depicted by the yellow square in **(F)** revealed holes in the membrane reaching deep inside the cell (arrow). AP: Action potential; APD_{90}: Action potential duration, calculated at 90% of repolarization; NRVM: Neonatal rat ventricular cardiomyocyte; PosNP: Positively charged, amine-modified polystyrene latex nanoparticle.

Europe PMC Funders Author Manuscripts

Europe PMC Funders Author Manuscripts

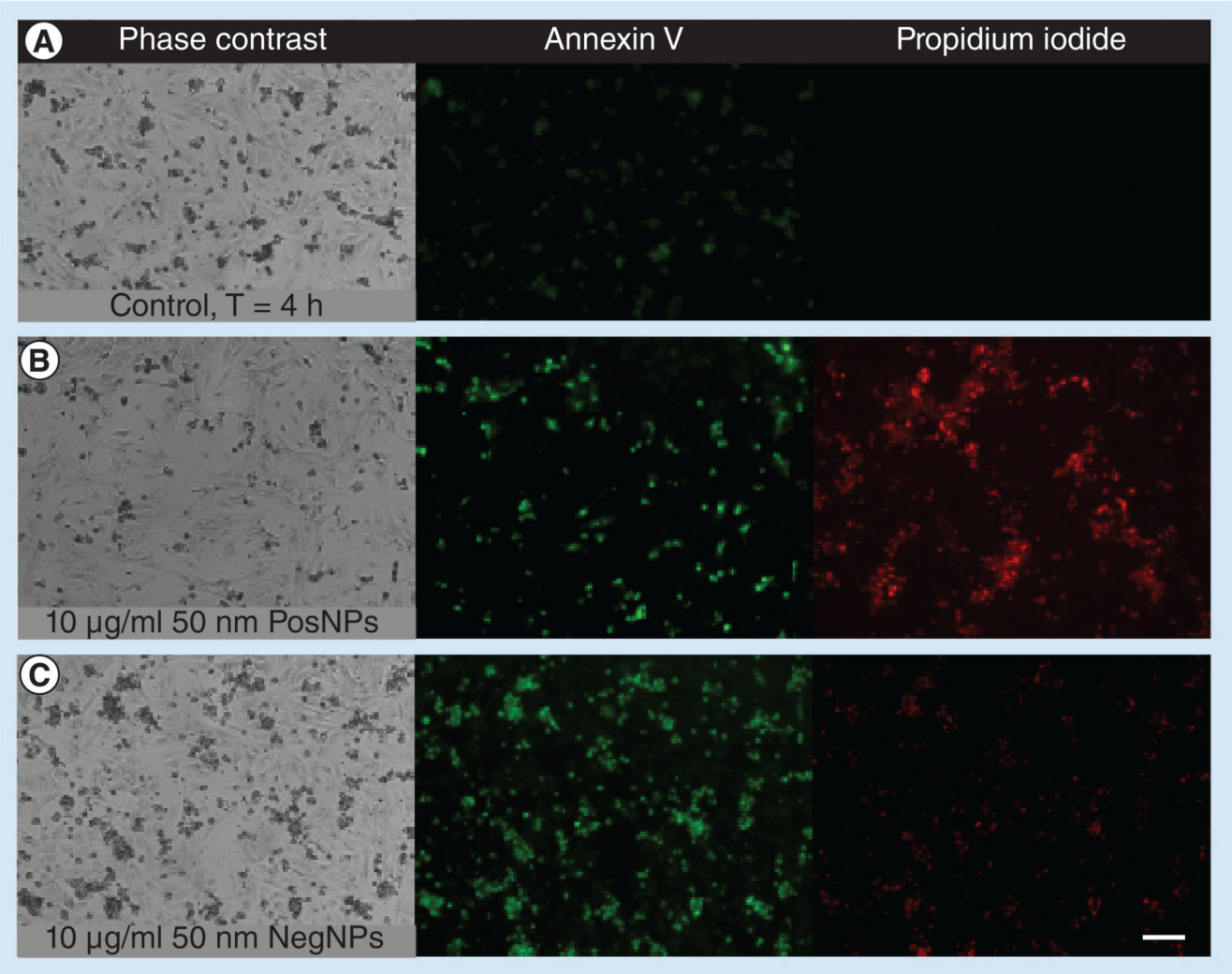

Figure 3. Effect of positively and negatively charged nanoparticles on cell life.

Fluorescent micrographs show typical apoptotic features in neonatal rat ventricular cardiomyocytes exposed to 10 µg/ml of 50 nm **(B)** PosNPs or **(C)** NegNPs for 4 h before staining with annexin V (green) and propidium iodide (red) compared with the control **(A)**. Both particles induce annexin V. By contrast, only PosNPs induce significant propidium iodide uptake, a marker of necrotic cell death. Scale bar = 100 µm.

NegNP: Negatively charged, carboxyl-modified polystyrene latex nanoparticle; PosNP: Positively charged, amine-modified polystyrene latex nanoparticle. For color images please see online www.futuremedicine.com/doi/pdf/10.2217/nnm.12.125.

Europe PMC Funders Author Manuscripts

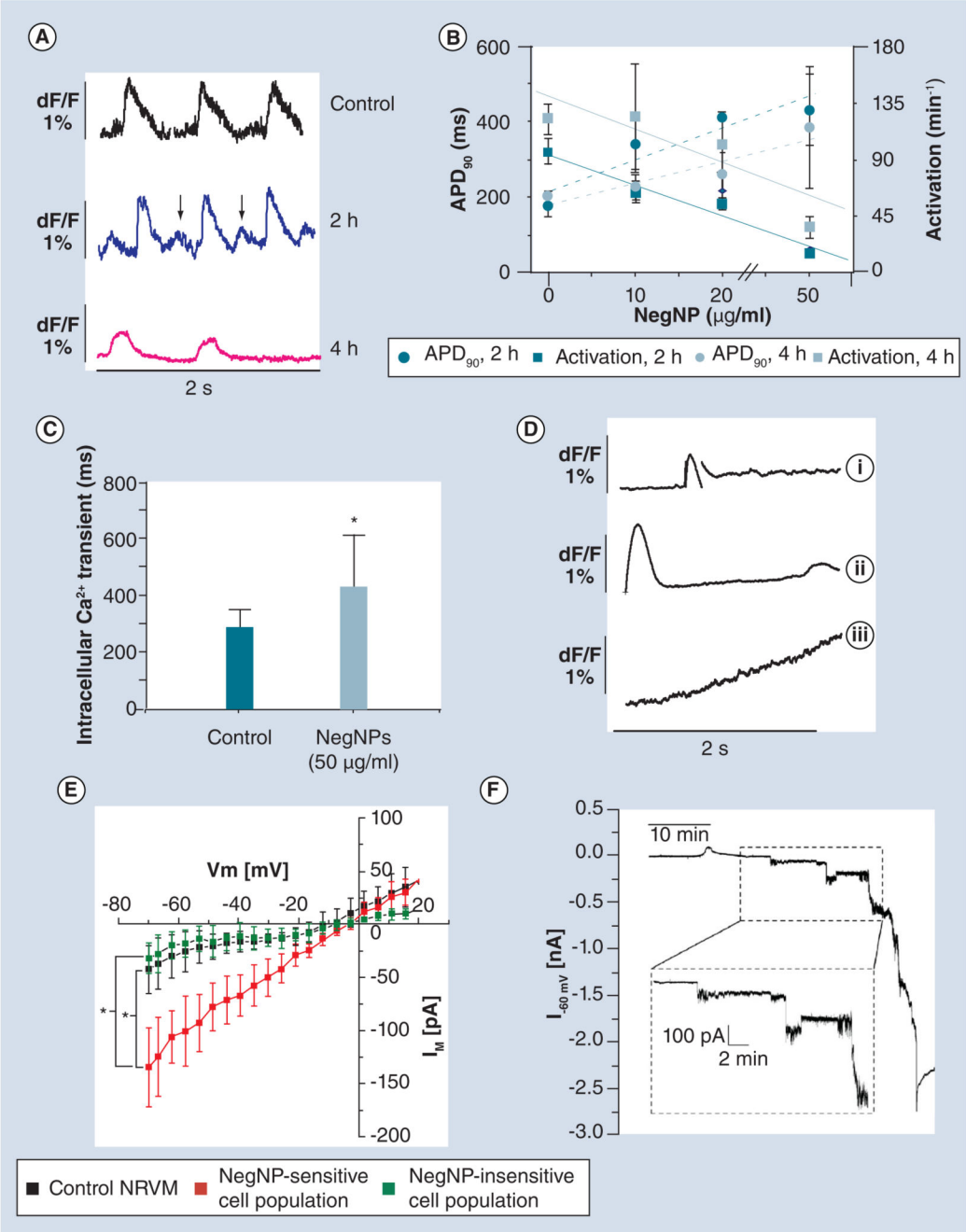

Figure 4. Electrophysiological characterization of the interaction between negatively charged, carboxyl-modified polystyrene latex nanoparticles and neonatal rat ventricular myocytes.

(A) Optical action potential recorded at time 0, 2 and 4 h following 50 μg/ml NegNP exposure. Of note, after 2 h, delayed afterdepolarizations are often observed (arrows). **(B)** Dose-dependent linear relationship between APD_{90} (dotted lines) and spontaneous activities (solid lines) following 2- and 4-h NegNP exposure ($r^2 = 0.86$ for both; n = 10; mean ± standard deviation). **(C)** Optical Ca_i^{2+} transient duration before and after 2-h exposure to 50 μg/ml NegNPs (n = 45; *$p < 0.05$). **(D)** The Ca_i^{2+} transient for the three groups measured in

single neonatal rat ventricular myocytes (NRVMs) exposed to 50 μg/ml NegNPs: **(i)** Affected Ca^{2+} re-uptake, **(ii)** one prominent Ca^{2+} transient, followed by a delayed smaller transient, and **(iii)** gradual Ca^{2+} increment, during the entire recording period (n = 19 cells per group). **(E)** Steady-state membrane current/voltage characteristics (I_M/Vm) of control NRVMs and after 2-h exposure to 10 μg/ml NegNPs. The NegNP-sensitive and NegNP-insensitive cell populations are shown (*$p < 0.05$ in the I_M current at a potential of -70 mV in the figure). **(F)** Example of 50 min recording of I_M of NRVM held at a pipette potential of -60 mV following acute exposure to 10 μg/ml NegNPs (n = 7).

APD_{90}: Action potential duration, calculated at 90% of repolarization; I_m: Net current across membrane; NegNP: Negatively charged, carboxyl-modified polystyrene latex nanoparticle; Vm: Membrane potential.

Europe PMC Funders Author Manuscripts

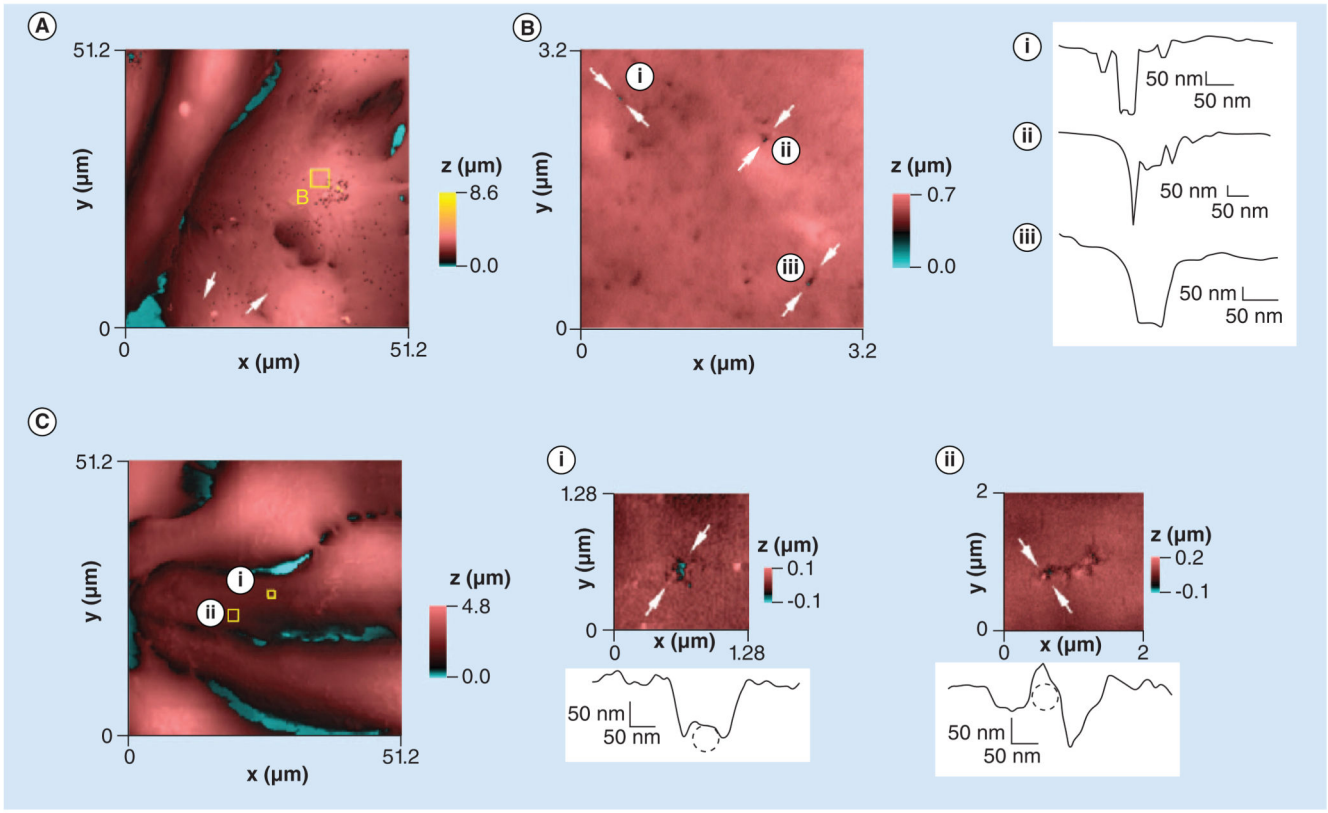

Figure 5. Hopping probe scanning ion conductance microscopy images and profile scans comparing fixed and live neonatal cardiomyocytes exposed to negatively charged, carboxyl-modified polystyrene latex nanoparticles.

(A) Height-coded color topography image (51.2 × 51.2 µm) of neonatal rat ventricular cardiomyocytes fixed and imaged by hopping probe scanning ion conductance microscopy after 4 h incubation with 50 µg/ml of negatively charged, carboxyl-modified polystyrene latex nanoparticles (NegNPs). **(B)** Left: high-resolution scan (3.2 × 3.2 µm) of area depicted by the square in **(A)**. **(B)** Right: height profiles across three different holes in the membrane (arrows marked **i–iii**) caused by exposure to NegNPs. **(C)** Live neonatal rat ventricular cardiomyocyte imaged by hopping probe scanning ion conductance microscopy after acute exposure to 10 µg/ml of NegNPs. **(Ci)** 1.28 × 1.28 µm area depicted by the square in **(C)** with a height profile of the membrane disruption in the direction marked by arrows. The 50 nm diameter dashed circle represents a nanoparticle trapped inside the damaged area. **(Cii)** High-resolution scan (2 × 2 µm) in the area depicted by a square in **(C)**, with a height profile of the membrane disruption in the direction marked by arrows. The 50 nm diameter dashed circle represents a single nanoparticle trapped in the disrupted area.

Europe PMC Funders Author Manuscripts

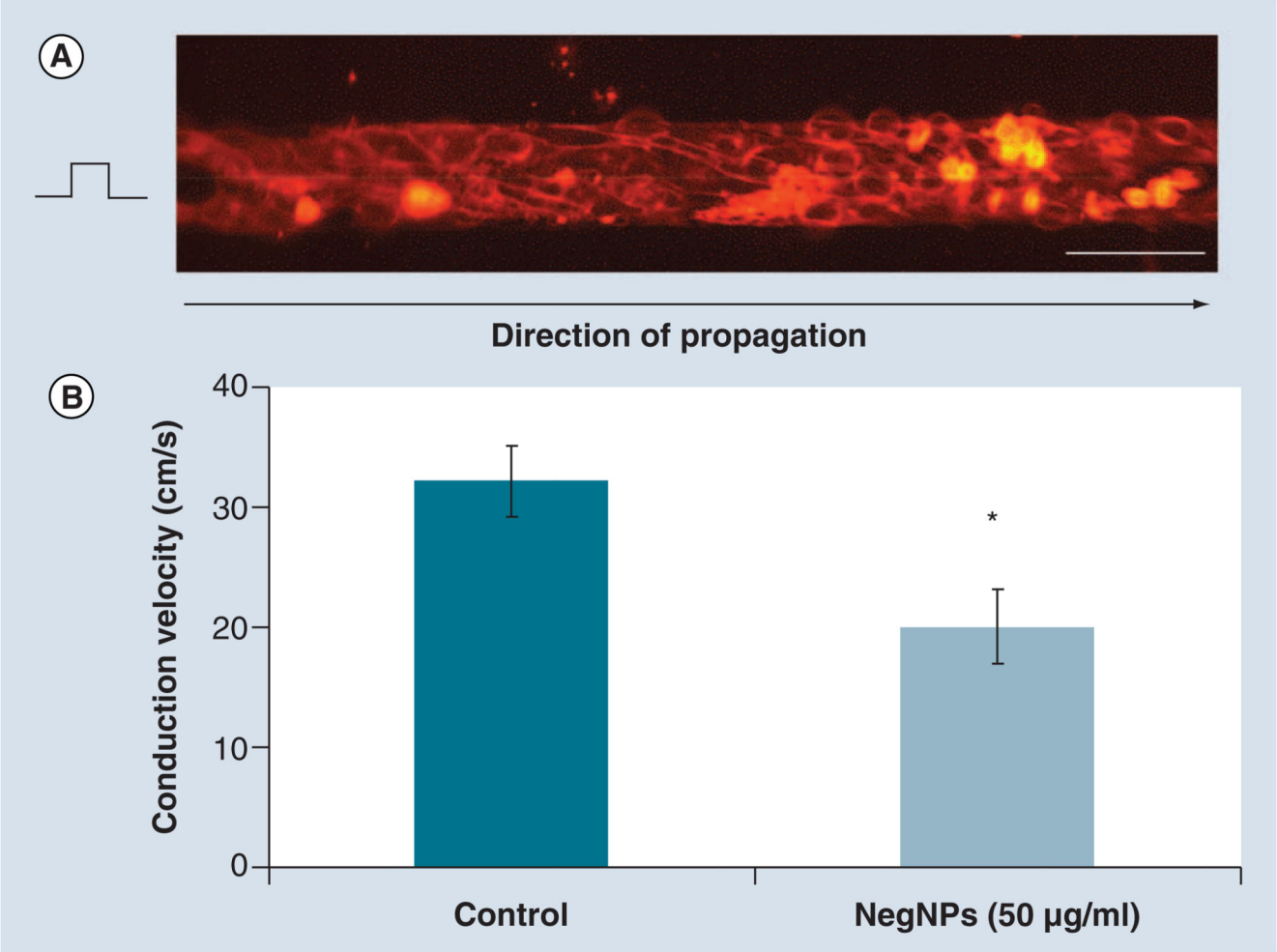

Figure 6. Cardiac impulse propagation in the presence of negatively charged, carboxyl-modified polystyrene latex nanoparticles.

(A) 80-µm width strands of neonatal rat ventricular cardiomyocytes stained with voltage-sensitive dye, Di-8-ANEPPS (scale bar = 100 µm). Strands were stimulated 1 mm from the left side to avoid artifacts and the impulse propagation was recorded along the field of view. **(B)** The conduction velocity was significantly reduced in strands exposed to 50 µg/ml of 50 nm NegNPs for 2 h (n = 10; mean ± standard deviation; *$p < 0.05$).

NegNP: Negatively charged, carboxyl-modified polystyrene latex nanoparticle.